Proceedings World Geothermal Congress 2020+1
Reykjavik, Iceland, April - October 2021

Geology, Geochemistry and Geophysical Geothermal Exploration in Paucarani Zone, Tacna, Peru

[1] Vicentina Cruz, [1] Rosmery Flores, *Diana Pajuelo

[1]INGEMMET, Av. Canadá Nº 1470, San Borja Lima 41, Perú, Apartado 889, * (formerly INGEMMET)

Email: vcruz@ingemmet.gob.pe, rflores@ingemmet.gob.pe, * dpajueloaparicio@gmail.com

Keywords: Geothermometers, Paucarani, Curimani,hot-spring, geothermal

ABSTRACT
The Paucarani geothermal zone (ZGP) is located in the Western Cordillera of the Andes of southern Peru. It is characterized by the presence of fumarolic vapor (solfataras) and thermal spring discharge associated to volcanic rocks (<3 Ma). These rocks overlie Mesozoic sedimentary rocks and Paleogene-Neogene volcanism controlled by the Incapuquio regional fault system and the dextral Paucarani fault, which exerts structural control of the volcanic rocks. The NW-SE lineaments established the boundary between the pyroclastic and epiclastic sequences, with the andesite-dacitic Barroso Group lavas. The last event corresponds to Paucarani volcano lavas (<1 Ma). The hot springs with surface temperatures between 17.2 °C – 81 °C, are classified into the following water types: Na-Cl, Ca.Mg-SO_4.Cl and Ca.Mg-HCO_3. The geothermometers estimated the reservoir temperatures to be <221 °C (SiO_2), <120 °C (K / Mg) and > 260 °C (Na-K-Ca). The fluid-rock interactions have not reached full equilibrium; probably due to an active magmatic system manifested by the presence of highly acidic fluids (with a strong smell of sulfurs). The pH of hot springs fluids shows variation from 1.5 to 8.7. The values of δ^2H and $\delta^{18}O$ indicate that the fluids originate from a mixture of magmatic fluid and meteoric water that infiltrates at a deep level by fault systems of NW-SE and ENE-WSW orientations.

The geophysical magnetotelluric method identified a conductive anomaly (<10 Ohm-m) from the surface to 2000 m depth. This is associated with the clay cap, with a thickness of 1200 m, and a resistive anomaly (8 -70 Ohm-m) with an average thickness of 1500 m linked to the reservoir. Also detected was a conductive anomaly from 7000 m depth, related to geothermal fluid ascent. Also identified was the presence of negative anomalies to the SW and SE of the study area, which is related to the geothermal flow associated with the fault system and fractures of NW-SW, EW and NE-SW orientation. The geological, geochemical and geophysical results were integrated to construct a conceptual model for the Paucarani geothermal system. This model indicates that the geothermal fluids are associated with magmatic sources. In addition, it was determined that for an area of at least 10 km^2, the geothermal potential is about 72 MWe with a 62% probability.

1. INTRODUCTION

The Paucarani geothermal zone (ZGP) is located on the Western Cordillera of the Andes in southern Peru. It is part of the mountain range of volcanic origin, named as the Cordillera Barroso (Siebert et al., 2010). The study area covers 600 km^2. Thermal waters discharge on the surface associated with tectonically active fault systems with recent volcanism (<3 Ma). Hydrographically, it belongs to the Uchusuma River basin. The volcanic and structural phenomena produced fractures and faults on volcanic rocks and basement; precisely, fractures and faults control the recharge, circulation and discharge of geothermal fluids, either in deep or superficial areas. Likewise, it has been observed that all the volcanic centers in the Tacna region have a regional structural control oriented NE-SW; faults are associated with surface geothermal manifestations (Cruz et al., 2013). Moreover, the geothermal manifestations in Paucarani have a juvenile origin with high temperatures (81 °C) and have a relation to heat sources from magmatic chambers associated with Holocene volcanism. The heat released by a magmatic source would be transmitted to the surface through deep faults (Cruz et al., 2013).

Geological, geochemical and geophysical studies on the surface were carried out in order to expand knowledge within the ZGP and to postulate a conceptual model. The integration of these multidisciplinary studies gave a better understanding of the geothermal system characteristics (Georgsson, 2009).

2. GEOLOGY, GEOCHEMISTRY AND GEOPHYSICAL STUDIES

2.1 Geology

The regional studies included the analysis between stratigraphic units and regional faults, and their interaction inside the ZGP. The rock mapping and geological structures control allowed identifying the lithology, faults and volcanic structures, such as volcanic cones and domes.

The ZGP is surrounded predominantly by volcanic rock outcrops and fluvioglacial deposits. The volcanic rocks are from Pleistocene (Barroso Group) and Holocene (volcanic cones and domes) ages. However, regional analysis indicates that volcanic units (Cenozoic ages) cover sedimentary and igneous rocks (Jurassic to Cretaceous ages). On the west side of ZGP, the oldest rock outcrops are exhumed and controlled by Incapuquio regional faults. The sequences vary from lavas interbedded with conglomerates (Chocolate Formation), limestones (Pelado Formation), and limestones, sandstones and silty claystone (Socosani Formation) of the Lower Jurassic. Next are sandstones - shales, sandstones - silty claystone, limestones-sandstones-shales (Yura Group) from Upper Jurassic ages and sandstones with quartz (Hualhuani Formation) from Lower Cretaceous. Sequences of andesitic and agglomerate of lavas (Matalaque Formation) from the Upper Cretaceous covers the previous sequences. Overlying are volcanic tuffs, siltstones and limestones (Tarata Formation) from Paleogene and tuffs interbedded with andesitic lavas (Huilacollo Formation) from the Miocene. The thicknesses of the Matalaque, Tarata and Huilacollo formations are 700 m, 250 m

and between 200 and 1000 m respectively (Monge & Cervantes, 2000). The sedimentary and volcanic sequences from Jurassic to Paleogene ages are cut by Miocene intrusive granodiorite rocks (Batolito Challamiento). On the other hand, the eastern zone of the ZGP presents Miocene volcanic outcrops of andesitic lava (Tacaza Group), sandstones and conglomerates (Maure Group) from Upper Miocene, Pliocene tuffs (Grupo Sencca) reworked sandstones, and also siltstones and conglomerates (Capillune Formation) from the Pliocene (Fig. 1A). The thicknesses of the Maure Group and Sencca and Capillune formations vary between 800 to 1200 m, and 80 to 200 m, respectively (Monge & Cervantes, 2000). The central sector of the ZGP contains outcrops of andesitic to dacitic volcanic rocks positioned as domes, later covered by unconsolidated deposits of fluvioglacial origin.

The ZGP is located in the middle of two blocks where the lithological composition varies. Thus, the oldest rocks are exhumed on the west, which is not seen on the east side. (Fig. 1B). The western zone contains the oldest rocks caused by deep fault systems that allow the exhumation of Jurassic age rocks (Incapuquio fault system). The andesitic and dacitic lavas of the Barroso Group cover lithological sequences previously affected by the movements of the faults. The location of domes in the central zone shows the recent volcanic activity on ZGP; therefore, the central zone is favorable for the emplacement of geothermal fluids.

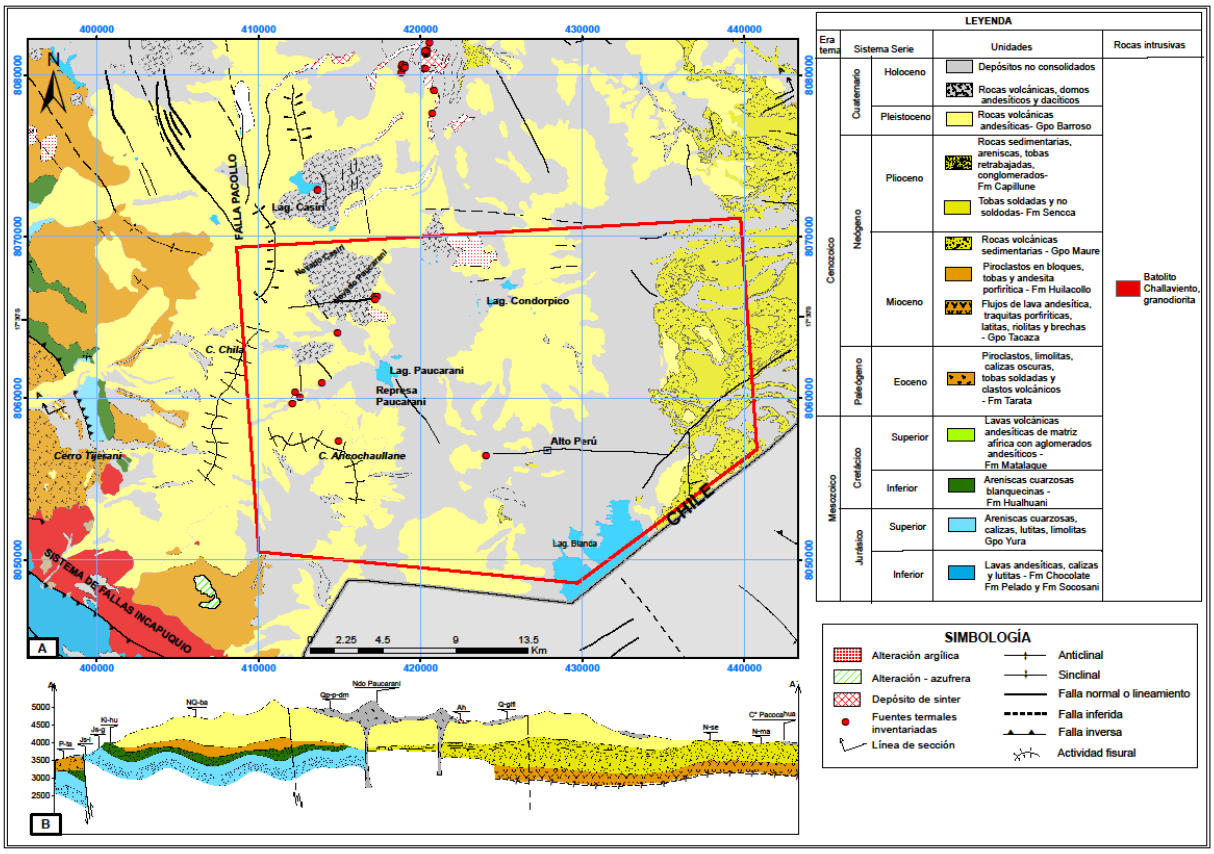

Figure 1. (A) Regional geology map of the ZGP and surrounding area. (B) Geological cross section (A-A´) between Potino and Pocahua hills.

The surface geology within the ZGP is different in the SW sector compared to the NE. The SW sector is characterized by the presence of surface manifestations, such as thermal springs and fumaroles. Lava rocks on the surface have andesitic to dacitic composition; however lavas are interbedded with homogeneous agglomerate layers and sandstone as a result of autoclastic processes and resedimentation. In this sector, a dome with NNE-SSW orientation, named as Cerro Blanco, have dacitic to rhyolitic composition and Holocene age. Similarly, the Nevado Paucarani consists of andesitic to dacitic lavas. A dome is located at the top, which results from the last volcanic event during the Holocene. The base of the Nevado Paucarani contains soil vaporizing surface emanations, which generate the sulfur crystallization. On the other hand, the NE sector presents the oldest sequences, which are located at the base of the Paucarani reservoir rocks. These consist of welded tuff (Sencca Formation) covered by tuffs and sandstones with conglomerate channels (Capillune Formation). These sequences are covered by andesitic lavas (Barroso Group) and fluvioglacial deposits. The difference in lithology on the surface between these two sectors limits a NW-SE trend where the Nevado Paucarani and Paucarani reservoir are located. The lithological difference in the surface suggests a fault that limits these two sectors. This is recognized as the Paucarani fault.

2.1.1 Structural analysis

The structural analysis was based on the processing of aeromagnetic geophysical information and structural data obtained in the field (fault planes, joints and fractures). The aeromagnetic geophysical analysis were completed in 2001 and the data were obtained from the Andean Multinational Project (PMA) in Bolivia, Chile and Peru. The structural data was obtained from the field campaigns carried out with the Geothermal Project (INGEMMET) and collected around thermal manifestations.

a) Magnetic data analysis

According to the reduction to the pole technique, a magnetic map and lineaments were elaborated from the horizontal gradient and the total magnetic field. The field magnetic intensity has a range between -744 to 1146 nT. The inclination of the Earth's magnetic field in the study area is approximately -8.3; this value was used for processing, correction and data reduction. Figure 2A shows the reduction to the pole map from the aeromagnetic data for the ZGP area. Where there are contrasts between magnetic highs and lows, the positive values indicate the position of higher magnetization sources (Fanton et al., 2014). In the NW, the elongate magnetic anomalies are positive, controlled by lineaments with NW-SW direction. These anomalies reach maximum values up to 1186 nT. To the SW and SE, the anomalies are negative in an elongated area, limited by lineaments with NW-SW direction and minimum values of -744.43 nT. These anomalies have a relation with fluid flow that is structurally controlled by oriented fractures (NW-SW and EW), associated with the presence of geothermal manifestations (hot springs up to 81 °C, fumaroles, and mud pools) and by hydrothermal alteration by fluid-rock interactions (Hinze, 2013).

The magnetic lineament map (Fig. 2B) obtained from the horizontal gradient revealed the impartial representation of the measured data, smoothed the signal, and showed a double shading that revealed the trend of anomalous characteristics in one direction (Korhonen, 2005). For the ZGP, the magnetic lineaments were defined in three (3) directions: 1) NNW-SSE to NS of great extension and controlling the interest area, possibly related to regional faults, 2) NE-SW observed in a large amount, which would be the result of efforts generated by large regional faults, and 3) E-W in a smaller amount with smaller extensions. The lineaments with NE-SW and E-W direction probably have been produced by regional faulting, which would have a relationship with the porous and fractured rocks and allow the circulation and ascent of geothermal fluids in the ZGP.

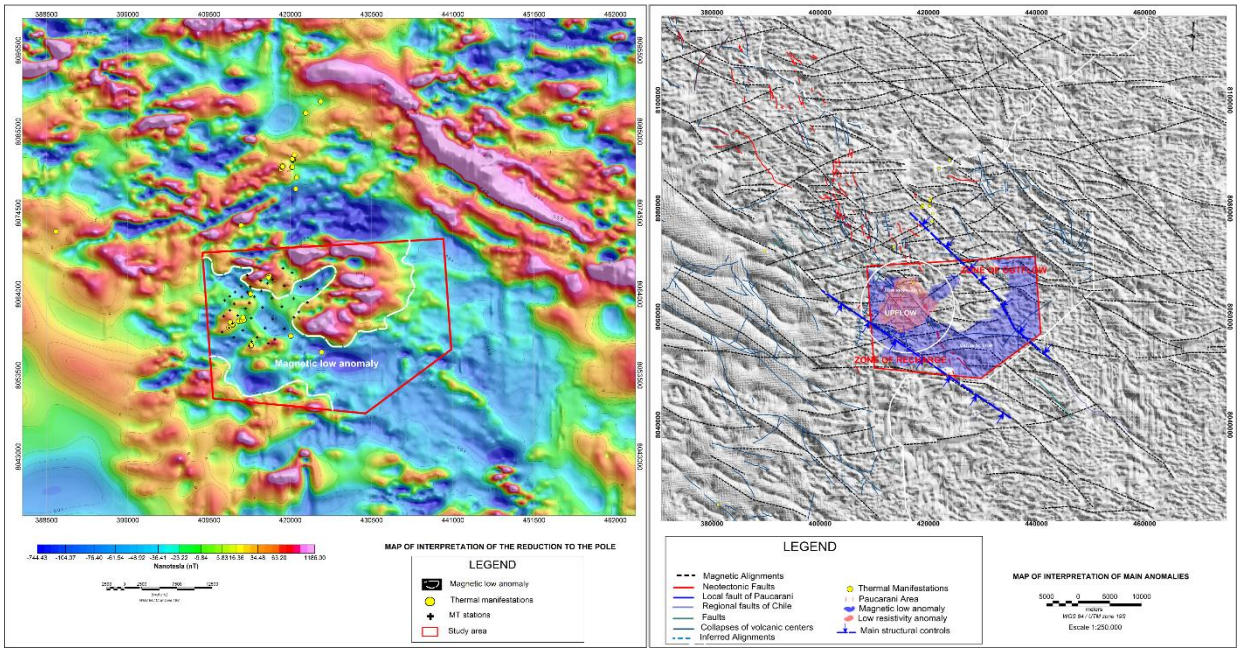

Figure 2. A) Reduction to pole technique. The map shows the low magnetic anomalies. B) Map of the magnetic technique interpretation, and resistance anomalies.

b) Field Structural data

The structural analysis was based on 20 stations of structural control in the ZGP (Fig. 3A). The data were taken predominantly to the surroundings of the thermal sources in rock outcrops. The structural data includes fault planes with grooves, fractures and veinlets. In the SW sector of the Paucarani reservoir, greater control data were located compared to the NE sector. The NE sector (Fig. 3A) presents diaclases and veins with NW-SE and NE-SW direction, an anticline axis with NE-SW orientation, sinestral heading faults, and normal SW convergence faults. The data collected in the SW sector present fault planes, diaclases and gap zones aligned in a NW-SE direction (Fig. 3A). The data collected are grouped to the south and north of the Curimani ravine, where the most thermal springs discharge.

Faults on the south of Curimani water creek:

The fault planes are located south of the Curimani ravine (Fig. 3A) in the outcrops of breccia (Cerro Ancochaullane, between 4915 and 5107 m a. s. l.), which are cut transversely and lightly. The data were recorded in structural stations 19 and 20, processed with the Faultkin 7 software (http://www.geo.cornell.edu/geology/faculty/RWA/programs, Fig. 3A). Faults have dextral type component volcanism, and the component varies as normal and inverse. The fault planes are of short route and cut the sequences of gaps located in the Barroso Group. In the case of station 19, the fault plane has azimuth with orientation 82° to 120° and a 90° plunge. Stretch measurements were taken in the fault mirror, being 22° to the east of the average of the pitch. Therefore, the

kinematics of the fault is dextral with an inverse component, and the effort is transpressive. The aforementioned faults do not have a long length. In the case of station 20, it has azimuth with orientation 185° to 190° and plunge between 82 ° and 90 ° to the east; the average pitch of the stretch marks varies between 20° and 50° to the north. The kinematics of the fault is dextral with a normal component and the stress is transtensive.

According to rose diagrams, fracture systems have a similar trend compared with breccia outcrops, thus indicating that the distention axis would be perpendicular to the joint direction. The distensive fault strength stimulates the fluid migration through the surface because it represents an area of greatest weakness. The stress-strain diagram shows that the main axis (σ1) has a NW-SE direction and the least effort (σ3) has a NE-SW direction, which is similar with the NW-SE breccia outcrops and fold axis with NE-SW direction generating transpresive strength.

Faults on the north of Curimani water creek:

Faults in Llavimocco hills at the north side of Curimani generate a graben. The bottom of the graben contains hot springs and fumaroles which form mud pools (Fig. 3A). A ramp with SE-E direction contains volcanic rocks and soft folds; the tectonic movement generates breccia with volcanic and silicified clasts.

The bottom of the Paucarani Mountain has an anticline fold with 40º trend. Fractures and oxide veins have 100º direction. Vapor infiltrates through joints and precipitates sulfur crystals. Therefore, the main axis of effort (σ1) has NW-SE direction and the lowest axis (σ3) has a direction of NE-SW. The microtectonic analysis develops structures inside a transpressive and transtenssive conditions, which correspond the accommodation with ancient structures.

The ZGP contains structures with high angle, in general, and the structure orientation determines a transpressive system dextral type. Also, the regional orientation is NW-SE along the Paucarani reservoir. The transtension model is comparable with structural data found inside the ZGP.

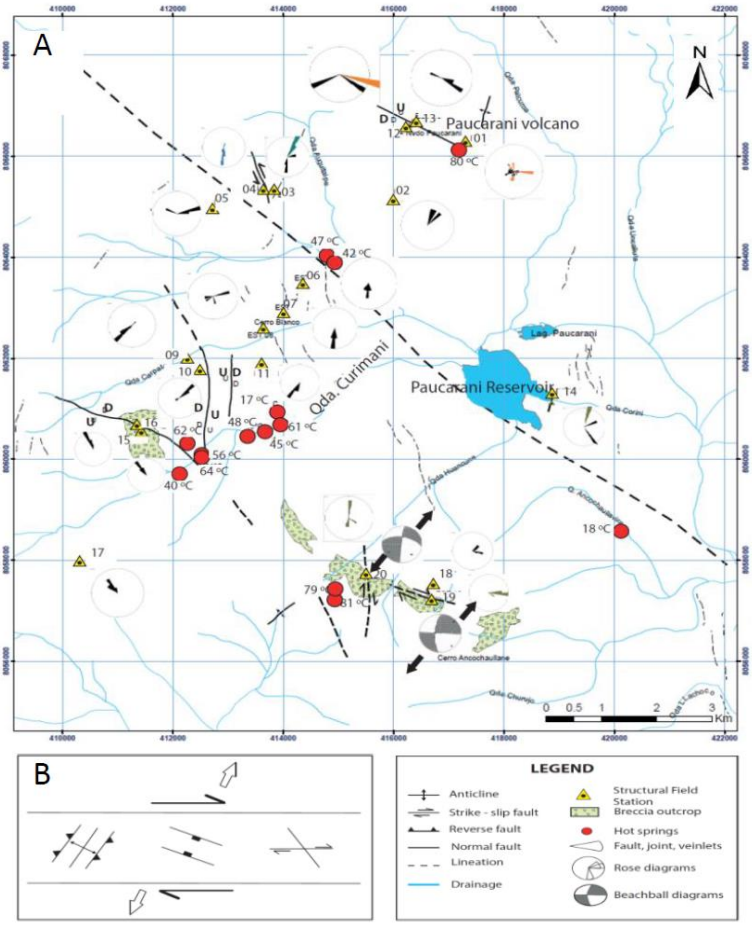

Figure 3. A) Structural map at Paucarani geothermal zone. B) Schematic model of Paucarani structural controls.

2.2 Geochemistry

Samples were collected from 63 sets of hot and cold water between May and September of 2017. From each source, 3 samples were collected: one for the analysis of dissolved cations (Li, Na, K, Ca, Mg, B, As, Si and trace elements) after filtration through a 0.45 µm Millipore filter was acidified using ultra-pure HNO_3; and a second one was taken without acid addition, to determine anion composition (Cl, F, Br, SO_4 and CO_3, HCO_3) (non-preserved sample). A third sample was used to determine the isotopic composition. These samples have allowed establishing a baseline to explain the thermal water chemistry (Giggenbach and Goguel, 1989, Marini, 2000). During the sampling, the parameters of the outlet temperature (± 0.1 °C), pH (± 0.1 units) and electrical conductivity were measured using multiparameter equipment (WTW 340I).

The sample analyses were carried out in the INGEMMET and ALS S.A.C. (with ISO / IEC 17025 accreditation) laboratories. The analyses were as follows: 1) dissolved metals and trace elements (Li, Na, K, Ca, Mg, B, As, Si) by ICP-OES Varian 735-ES Radial and ICP-MS Nexion 300D, Perkin Elmer (EPA Method 200.7 and EPA Method 200.8), 2) Cl, F, Br, SO_4 by ion chromatography using a Dionex ICS-2000 chromatograph and (3) HCO_3 was analyzed volumetrically by titration with 0.1 N HCl. The accuracy and precision were verified with certified materials making several replicates and sample dilutions. The analytical errors were less than 10% (Murray and Wade, 1996). The isotopic analysis (δ^2H and $\delta^{18}O$) was performed by ICP-MS Delta S in the LaGeo laboratory (with ISO/IEC 17025 accreditation) at El Salvador.

a) Water chemistry

The thermal and cold water within ZGP have temperatures between 5.8 to 81 °C, and pH from 1.5 to 8.76. The pH < 4.5 belongs to waters from hydrothermal alteration areas at high altitudes above 4800 m a.s.l. The electrical conductivity (EC) ranges from 28 to 6090 µS/cm (the complete physio-chemical data could be found in http://www.ingemmet.gob.pe/gegramamia-program1). The high EC value corresponds to the Paucarani lagoon, which has acid pH (3.85), and is associated to lateral outflow that blends Nevado Paucarani fluids (fumaroles located at 1km to SE of the dome) with meteoric water. Leaching and evaporation processes increase the ammount of ions dissolved in the water.

The hydrochemical classification was based on the water samples distribution using the Langelier-Ludwig diagram (Langelier and Ludwig 1942, Fig. 4A) and the ternary diagram proposed by Giggenbach (1988, Fig. 4B), diagrams show the following results. 1) Waters with temperatures <17 °C plot in the Ca.Mg-HCO_3 and Ca-SO_4 sectors, associated with H_2S oxidation processes and/or $CaSO_4$ leaching. 2) The hot spring waters are located in three sectors, Na-Cl, Ca- SO_4 and Ca.Mg-HCO_3. The Na-Cl waters discharge in Curimani water creek. Curimani waters possibly derive from Halita dissolution (water-rock interaction) or the water circulates in deep levels associated to high enthalpy systems (Nicholson, 1993; Marini, 2000). At a shallow level, they are mixed with volcanic fluids. 3) Waters from acid mud pool and volcanic condensate produced mixed sulphate water types (Na-SO_4, Ca-SO_4), which due to the high SO_4 composition indicates their association with volcanic fluids (fumarolic gases with H_2S odor).

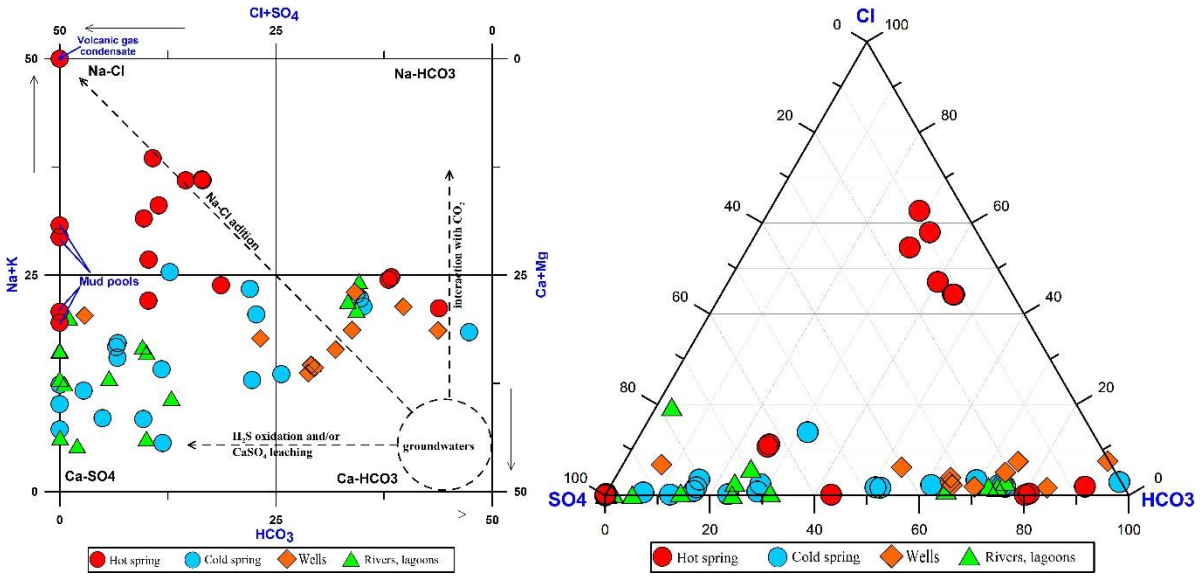

Figure 4. A) Langelier – Ludwig diagram. B) Relative amount of Cl, SO_4 and HCO_3.

The HCO_3 waters located to the S-SW of the Nevado Paucarani would be associated with volcanic activities. The CO_2 magmatic origin at different temperatures and at high pressures remains in solution in the hydrothermal fluid. Once the temperature declines below 330 ºC, the CO_2 (aq) becomes reactive and produce alteration around the aquifer host rock, while precipitating calcite and bicarbonate. These precipitates dissolve in low salinity waters, increasing the HCO_3 as the temperature decreases. The El Ayro wells waters (HCO_3) are associated with water rock interaction processes. The mixed water composition in this zone has a lateral outflow with NNW-SE direction. Waters come from Huancune, Curimani, Barroso and Nevado Paucarani areas to the Laguna Blanca. Water flows on surface and underground, influenced by Uchusuma water creek and fault system.

The Cl-Li-B ternary diagram (Giggenbach, 1991a, Fig. 5A) shows that thermal waters are distributed in three main fields. 1) Waters that come from older hydrothermal systems with absorption of low B/Cl steam. In this sector samples have low or no B. 2) Waters that originate from younger hydrothermal systems with vapor absorption and high B/Cl ratio, probably associated with the Nevado Paucarani hydrothermal system. 3) Waters with loss of Li or B and Cl absorption, where Cl and B are added to the Li solutions with similar proportions as crustal rocks.

The Li-Rb-Cs ternary diagram (Giggenbach and Goguel, 1989, Fig. 5B) contains cold, meteoric, and thermal waters that plot with characteristic components, such as Cl, B, Li, Rb and Cs that are mixed because of water-rock interaction processes (Giggenbach,

1991). Most hot and cold springs are plotted in Rb and Cs corners. However, more than 50% of the hot springs are located toward the Cs corner. From this, water during their ascent towards the surface could decrease the Rb element associated with secondary mineralization processes, where the Rb is absorbed by the Illita and K-feldspar, incorporating the Rb in their crystalline structure at temperatures > 300 °C. The Li is absorbed in precipitates of secondary quartz, micas or chlorite. Waters plotted towards the Rb corner have similar composition compared to crustal rock composition. The water discharge in the Curimani sector has high relative Rb content and high indicated Na/K and K/Mg temperatures (Fig. 6A, 6B) but non-equilibrium water-rock interaction, due to the samples being affected by secondary processes.

The well water (36x-AGT-18) that discharges in the Laguna Blanca is plotted toward the Li corner in the region where the Cs is absorbed in zeolites at temperatures <300 °C. In general, the hot and cold waters are outflow discharge, favored by the fault system (NE-SW) and fractures inside the study area.

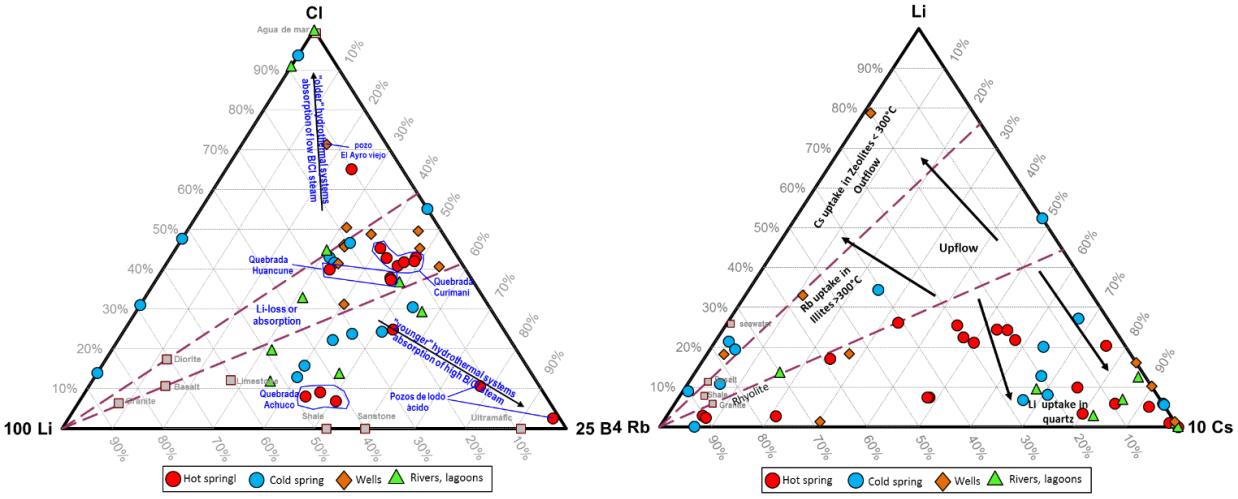

Figure 5. A) Cl-Li-B Ternary diagram. B) Li, Rb y Cs relative amounts.

b) Geothermometers

Using solubility chemical geothermometers of silica (quartz) (Fournier and Potter II, 1982), temperatures <125 °C were estimated with amorphous SiO_2 and beta cristobalite. With conductive quartz, temperatures were estimated up to 221.70 °C. The ion exchange geothermometers, such as Na-K-Ca (Fournier and Truesdell, 1973), Na-K-Ca-Mg (Fournier and Potter II, 1979, and Nieva and Nieva, 1987) and K-Mg (Giggenabach, 1986), estimated temperatures <265 °C. This value is unrealistic because of non-equilibrium water-rock interactions, possibly by the effects of interaction of the waters with rock at shallow depths, or by steam heating and associated acidification through oxidation of H_2S (Giggenbach and Glover, 1992). The diagram 10Mg / (10Mg + Ca) vs 10K (10K + Na) (Fig. 6A) shows this anomaly. Waters are located in the rock isochemical solution region by leaching processes (Giggenbach, 1988). Also, in the ternary diagram of Giggenbach, 1988 (Fig. 6B) thermal waters are plotted near the Mg corner in the immature waters sector. The waters with high Mg amount produced for the mixture with meteoric waters that infiltrate from high altitude areas, and temperatures are less than 100 °C. Also, their high Mg contents point to water-rock interaction under conditions far from equilibrium involving dilute, "immature" waters, possibly affected by the absorption of CO_2 or oxidation of H_2S (Giggenbach and Glover, 1992).

c) Stable isotopes

The stable isotopes values of δ^2H and $\delta^{18}O$ represented in Figure 7 shows that 85% of the waters are grouped over and near the Global Meteorological Line (LMG) (Craig, 1961) and 15% align far away. These correspond to Casiri and Paucarani Lagoons waters, indicative of experiment evaporation processes. Also, three samples of thermal water are observed in the direction of the andesitic water line; these waters discharge in the Huancune and Llavemoco sector as a result of the mixing between meteoric water with magmatic fluids. Hence, these waters are acidic. The values of δ^2H ranging from -58.1 ‰ to -133.6 ‰ and $\delta^{18}O$ ranging from -17.67 ‰ - 3.76 ‰ shows that the geothermal fluids in the study area originate from the meteoric water and magmatic water mixing. The heat source would be associated with Quaternary volcanism.

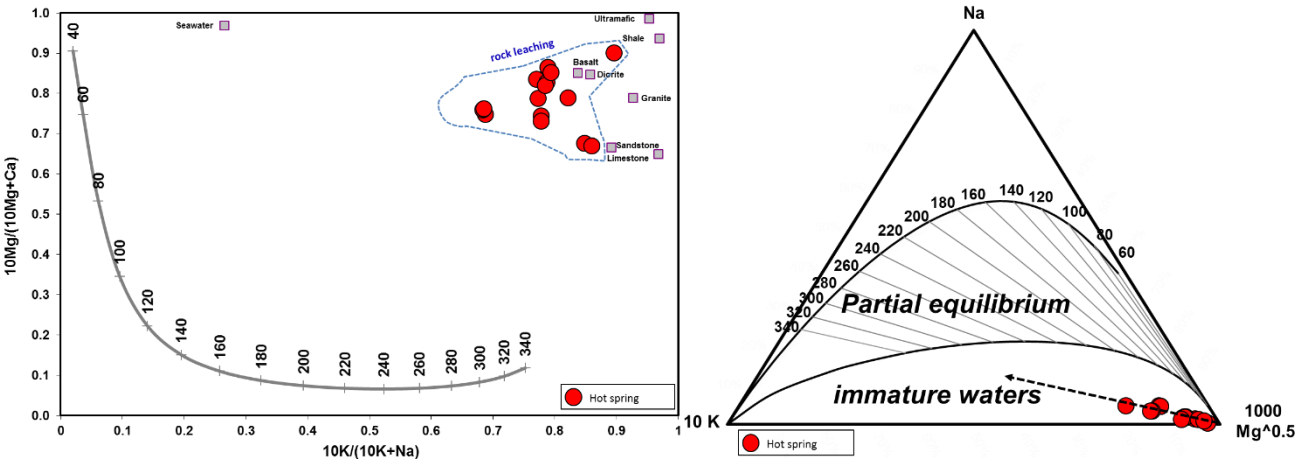

Figure 6. A) Geoindicador de Na-K/Mg-Ca. B) Ternary diagram.

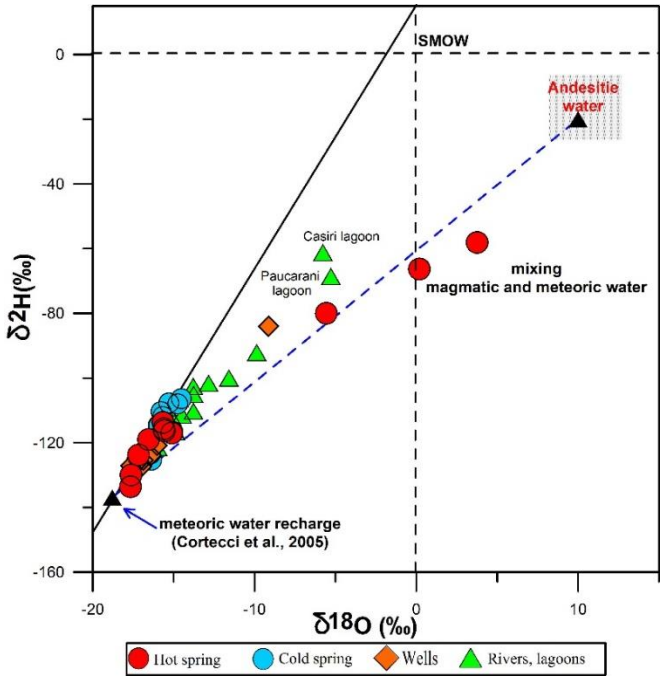

Figure 7. δ^2H vs $\delta^{18}O$ in the ZGP.

2.3 Geophysical

The magnetotelluric (MT) method was applied in an area of 120 km^2. The information was recorded with the Phoenix Geophysics MTU5A-System 2000 equipment in 46 stations. The pre-processing analysis was made using Phoenix Geophysics and WinGlink software for the 2D inversion. In addition, the conceptual model was interpreted in 2D profiles with SW-NE orientation.

2.3.1 Magnetotelluric Analysis

The data were inverted for three, two-dimensional models in the SW-NE direction. Perpendicular to the main geoelectric strike direction (NW-SE), the profiles allowed for the determination of the geometry and extension of the main elements of the Paucarani geothermal system. Profile 1 shows: 1) a superficial conductive anomaly (<10 Ohm-m) extended from the surface to approximately 2000 m depth, which is related to the clay cap with a thickness of 1200 m; 2) a resistive stratum underlying the clay cap from 2000 to 4000 m depth with resistivity values between 8 Ohm-m and 70 Ohm-m and a thickness averaging 1500 m; 3) a deep conductive anomaly from 7000 m, probably associated with an ascending zone related with the structural system; and 4) the estimation of a heat source at a depth > 10000 m.

Profiles 2 and 3 underline low resistivity anomalies, which allow determining the location of the geothermal system clay cap. The drastic changes in resistivity correlate with inferred faults analyzed on the surface with NW-SE orientation. The faults are the permeable zone for the geothermal fluids ascending from the heat source at depths > 9000 m. These would act as a system barrier towards the SW, related with the L5-38 and L6-44 stations. Profile 2 shows electrical resistivity located at 1000 m, 2000 m, 3000 m and 4000 m depth. The analysis displays a resistive anomaly in the center area at 1000 m depth, and extending in the NE-SE

direction. At 4000 m depth, the anomaly has a null extension, which indicates the presence of low porosity rock with low fluid. The anomaly with resistivity >10 Ohm-m extends toward SW of the study area. Based on geophysical results, a conceptual geophysical model was developed (Fig. 8).

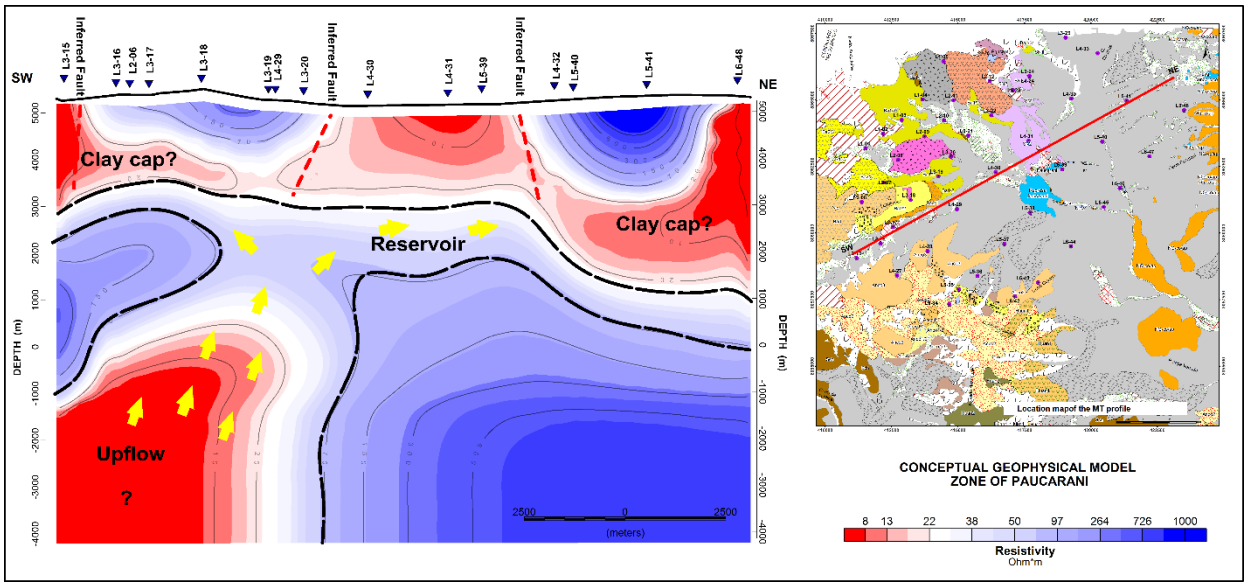

Figure 8. Conceptual geophysical model (Perfil SW-NE) for the Paucarani geothermal zone.

3. CONCEPTUAL MODEL AT ZGP

The conceptual model for the ZGP was elaborated on the basis of geological, geochemical and geophysical data. Data were integrated by superposition of layers, through techniques of Geographic Information Systems (GIS). Table 1 and Figure 9 show the relevant factors contributed by geology, geochemistry and geophysics disciplines, which allows estimation of the geothermal system of the ZGP.

Table 1. Geoscientific characteristics of the geology, geochemistry and geophysics to elaborate the geothermal conceptual model in ZGP.

Geoscientific aspects			
Conceptual geothermal model elements	**Geology**	**Geochemistry**	**Geophysic**
Heat source	Hydrothermal and magmatic activity (<1 Ma) in the Nevado Paucarani, Cerro Blanco and Cerro Huancune.	Fumarolic gas of magmatic origin, mud pools acid with H_2S odor and thermal waters (81 °C).	Through the magnetotelluric survey, is assumed the depth to> 9000m toward NW-SE.
Reservoir	Possibly between Huilacollo Formation and Toquepala Group, recognized on the western flank of the Cordillera del Barroso.	Quartz geothermometer <221°C Cationic geothermometer (Non-equilibrium water/rock interaction) temperature average <122°C.	Resistivity between 8 Ohm * m and 70 Ohm * m from 2000 m depth.
Flow patterns	NW-SE fault system along Paucarani dam.	Na-Cl, Ca-SO_4 y Ca.Mg-HCO_3 Langelier-Ludwig and ternary diagrams (Cl= 634.5mg/L).	Non apply
Clay cap	Geological unit of the Tacaza Group identified with the regional geology.	Non apply	Resistivity <10 Ohm * m, from surface to 2000 m depth.
Discharge zone (outflow)	Curimani, Huancune y Achuco ravines.	Mud pools (H_2S, Ca-SO_4), fumarolic gas (H_2S), hot springs (Ca-SO_4, Na-Cl).	It is located NW and SE associated with the main magnetic guidelines and geological structures and a possible discharge to the SW.
Fluid ascent zone (upflow)	Faults along (NW-SE) of the Paucarani dam.	Fumarolic gas condensate and mud pools of pH 1.5, temperature 80.1°C and high SO_4 (1150 mg/L).	Resistivity drastic changes in correlate with NW-SE inferred faults detect by geological studies.
Recharge zone	The mountain chain of Barroso, Nevado Paucarani and Condorpico mountain.	Isotopes δ^2H (-66.30‰) y $\delta^{18}O$ (0.19‰).	Non apply

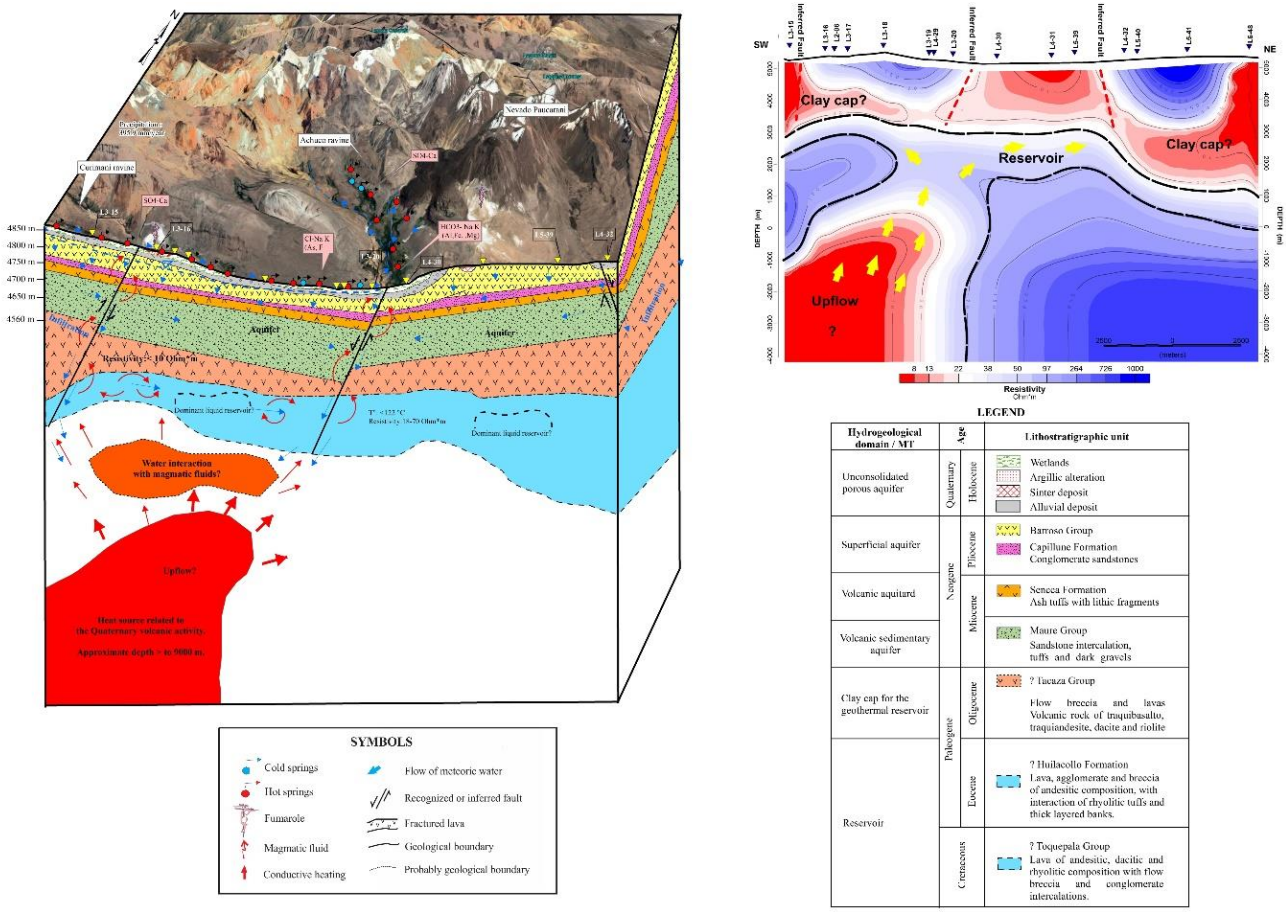

Figure 9. Geothermal resource conceptual model in ZGP using surface exploration data.

4. CONCLUSIONS

The ZGP is located inside a highly fractured and faulted zone, which allows for domes of Holocene age outcrops. In the Paucarani reservoir, a NW-SE lineament was identified that limits two zones with different lithology. This would represent a fault zone that is clearly identified with the magnetotelluric studies. The Paucarani fault generates movement between the lithological sequences, but in the SW sector displays distensive evolution, which allows the thermal sources to discharge.

According with chemical composition in ZGP, the hot and cold waters define basically Na-Cl, Ca.Mg-SO_4.Cl and Ca.Mg-HCO_3 water types, but the ionic domain is SO_4 and HCO_3. The Cl waters only discharge in the Curimani creek. The stable isotope relationship between δ^2H and $\delta^{18}O$ suggest that the geothermal waters are a mixture of meteoric and magmatic fluids. The ZGP contains at least one high-temperature reservoir below the Paucarani area with a possible temperature range of 120-200 °C.

The magnetotelluric method shows the resistivity model in Paucarani with three main indicators of the system: 1) a conductive layer at a depth of 2 km that plays the role of the clay cap; 2) the conductive zone interpreted as the reservoir to a relative depth between 2 and 4 km, which is possibly formed between the geological units of the Huilacollo Formation and Toquepala Group; and 3) a heat source of the geothermal reservoir in the SW direction of the Nevado Paucarani, which is interpreted as a magma intrusion located at > 9 km depth.

The estimated geothermal potential for the ZGP is 72 MWe for a minimum area of 10 km^2. There is a 62% probability for the use of the resource. However, the results should be checked with drilling.

ACKNOWLEDGEMENT

This work stems as part of a geothermal studies programme of the Instituto Geologico Minero y Metalurgico (INGEMMET, Peru). This institution financed the chemical, isotopic, mineralogical and dating analysis of the samples.

REFERENCES

Craig, H. (1961) - Isotopic Variations in Meteoric waters. *Science*, 133(3465): 1702-1703.

Cruz, V.; Vargas, V. & Cacya, L. (2013) – Caracterización y evaluación del potencial geotérmico de la región Tacna. *INGEMMET, Boletín, Serie C: Geodinámica e Ingeniería Geológica*, 56, 177 p.

Cruz V., Pajuelo D., Velarde Y., Flores R., Yupa G. (2017) - Caracterización y evaluación del potencial geotérmico en la zona geotermal de Paucarani, región Tacna. Informe técnico. Disponible en http://www.ingemmet.gob.pe/programa-de-geotermia1.

Fanton, G.; Martínez, P. & Giménez, M. (2014) - Procesamiento y análisis cualitativo de datos aeromagnéticos con vistas a la exploración de yacimientos hidrotermales tipo lode gold - provincia de La Rioja, Argentina. Geoacta, 39 (1): 30-50.

Fournier, R.O. & Truesdell, A.H. (1973) - An empirical Na-K-Ca geothermometer for natural waters. *Geochimica et Cosmochimica Acta*, 37(5): 1255-1275.

Fournier, R.O., and Potter R. W.II. (1979) - Magnesium correction to Na-K-Ca geothermometer. Geochim. Cosmochim. Acta, 43, 1543-1550.

Fournier, R.O., and Potter, R.W. II, (1982) - An equation correlating the solubility of quartz in water from 25 °C to 900 °C at pressures up to 10000 bars. *Geochim. Cosmochim.* Acta, 46, 1969-1974.

Georgsson, L.S. (2009) - Geophysical methods in geothermal exploration. *Short Course on Surface Exploration for Geothermal Resource*s, UNU-GTP and La Geo, El Salvador.

Giggenbach, W. F. (1986) - Graphical techniques for the evaluation of water/rock equilibrium conditions by use of Na, K, Mg, and Ca contents of discharge waters: P*roceedings* of Eighth New Zealand Geothermal Workshop, Auckland, New Zealand, p. 37-43.

Giggenbach, W.F. (1988) - Geothermal solute equilibria; derivation of Na-K-Mg-Ca geoindicators. *Geochimica et Cosmochimica Acta*, 52(12): 2749-2765.

Giggenbach, W.F. & Goguel, R.L. (1989) - *Collection and analysis of geothermal and volcanic water and gas discharges*. 4a. ed. Petone (New Zealand): Department of Scientific and Industrial Research, Chemistry Division, 81 p., Report CD-2401.

Giggenbach, W.F. (1991) – Chemical techniques in geothermal exploration. En: D'Amore, F., coord. *Applications of geochemistry in geothermal reservoir development*. Rome: UNITAR/UNDP Centre on Small Energy Resources, p. 119-144.

Giggenbach, W.F. (1991a) - Chemical techniques in geothermal exploration. En: D'Amore, F. (Ed.), *Applications of Geochemistry in Geothermal Reservoir Development*. UNITAR/UNDP Centre on Small Energy Resources, Rome, Italy, pp 119–144.

Giggenbach, W.F., and Glover, R.B. (1992) - Tectonic Regime and Major Processes Governing The Chemistry of Water and Gas Discharges From The Rotorua Geothermal Field, New Zealand, *Geothermics*, Vol 21, 121-140.

Hinze, W.J.; Von Frese, R.R.B. & Saad, A.H. (2013) - *Gravity and magnetic exploration: principles, practices and applications*. Cambridge: Cambridge University Press, 524 p.

Korhonen, J.V. (2005) - Airborne magnetic method: Special features and review on applications. En: Airo, M.L. *Aerogeophysics in Finland 1972-2004: Methods, system characteristics and applications*. Espoo: Geological Survey of Finland, Special Paper, 39, p. 77–102.

Langelier, W.F. & Ludwing, H.F. (1942) - Graphical methods for indicating the mineral character of natural waters. *Journal of the American Water Works Association*, 34(3): 335-352.

Marini, L. (2000) - *Geochemical techniques for the exploration and exploitation of geothermal energy*. Genova: Dipartimento per lo Studio del Territorio e delle sue Risorse, Università degli Studi di Genova, 82 p.

Mendivil, S. (1965) – Geología de los cuadrángulos de Maure y Antajave (hojas 35-x, 35-y). *INGEMMET*, Boletín, Serie A: Carta Geológica Nacional, p. 10, 99.

Monge, R. & Cervantes, J. (2000) - Memoria descriptiva de la geología del cuadrángulo de Pachía (36-x) y Palca (36-v), Escala 1:50 000. Lima: INGEMMET. 10 p.

Murray, K. & Wade, P. (1996) - Checking anion-cation charge balance of water quality analyses: limitations of the traditional method for non potable waters. *Water SA*, 22(1): 27-32.

Nicholson, K. (1993) - *Geothermal fluids: Chemistry and exploration techniques*. Berlin: Springer-Verlag, 278 p.

Nieva, D. & Nieva, R. (1987) - Developments in geothermal energy in Mexico, part 12—A cationic composition geothermometer for prospection of geothermal resources. Heat recovery systems and CHP 7, 243–258.

Siebert L., Simkin T., & Kimberley P. (2010) - *Volcanoes of the world*. University of California Press, Berkeley.

Torres, D; Muñoz, L.; Ayala, L.; Coba, L.; Martinez, J. & Cerpa, L. (2014) - Estructuras extensionales en un ambiente transpresivo durante el Mioceno inferior: Compatibilidad dinámica en el sistema de fallas Nazca, Puquio, Ayacucho, sur del Perú. En Congreso Peruano de Geología, 17, Lima, 2014, *Resúmenes extendidos*. Lima: Sociedad Geológica del Perú, 4 p.

Wilson, J. (1962) – *Geología de los Cuadrángulos de Pachía y Palca (Hojas 36-v y 36-x)*. INGEMMET. Boletín. Serie A: Carta Geológica Nacional, p. 4, 82.